Note: This thesis was prepared as an external research project (12 ECTS) during a student visit by Vicent Agustí Ribas Costa to the University of Helsinki. It is not a University of Helsinki Masters thesis.

Master's Thesis in Forest Sciences (12 ECTS)

Design and validation of a new technique for estimating canopy parameters: UAS-based spherical (360) photography, description of the forest canopy from inside.

Vicent Agustí Ribas Costa
Universidad Politécnica de Madrid (ETSIMFMN)
Department of Forest Sciences
Faculty of Agriculture and Forestry
University of Helsinki

Supervisor: Dr. Jon Atherton
Department of Forest Sciences
Faculty of Agriculture and Forestry
University of Helsinki

April 2021

Content

TITLE: Design and validation of a new technique for estimating canopy parameters: UAS-based spherical (360) photography, description of the forest canopy from inside.

AUTHOR: Vicent Agustí Ribas Costa

SUPERVISOR: Dr. Jon Atherton

DATE: April 2021

ABSTRACT: The canopy is a crucial part of the forests (light, carbon biomass… are parameters linked to canopy properties), and thus, always there has been interest in extracting information from it. One of the most used parameters is the Leaf Area Index (LAI, defined as one-sided leaf area per unit ground surface area). However, direct measurements of this parameter are destructive and not time efficient. Consequently, new indirect techniques were developed. One of the most used indirect techniques is digital hemispherical photography, an optical method that can derive LAI from gap fraction in the photographs taken of the canopy.

In this study, I analysed the potential of a UAS, the Parrot ANAFI, in estimating Plant Area Index, parameter related to LAI, but not corrected by clumping index nor woody material. This drone had two characteristics that make it ideal for forest parameter estimations: the capacity of taking spherical images and its size and weight, that allow it to be flown through the canopy.

Spherical images taken by the UAS were transformed into hemispherical ones, and were used to calculate PAI; simultaneously, photos of the same spot were taken with the traditional digital hemispherical equipment as validation data. Results showed a very high accuracy of the new method ($R^2 = 0.80$). Furthermore, vertical profiles of PAI were created by taking spherical images throughout the canopy height. Foliage density profiles were derived from those vertical profiles. Primary results also were promising.

KEY WORDS: Leaf Area Index, Plant Area Index, foliage density, Digital Hemispherical Photography, UAS, Parrot ANAFI.

Table of acronyms and symbols

UAV	Unmanned Aerial Vehicle
UAS	Unmanned Aerial System
DHC	Digital Hemispherical Camera
DHP	Digital Hemispherical Photography
LAI	Leaf Area Index
LAD	Leaf Area Density
PAI	Plant Area Index
PAD	Plant Area Density
$\boldsymbol{\alpha}$	Woody/non-woody ratio
$\boldsymbol{\gamma_E}$	Needle-to-shoot area ratio
$\boldsymbol{\Omega_E}$	Element clumping index
$\boldsymbol{\Omega}$	Clumping index
$\boldsymbol{P(\theta)}$	Gap fraction
$\boldsymbol{\theta}$	Zenith angle

Index of figures

Index of tables

1. INTRODUCTION

1.1. Background

When describing the forest canopy there are different parameters that are considered, but one of the most important variables to describe the canopy structure is the Leaf Area Index (Chen *et al.,* 1997). This parameter influences many biological and physical processes, such as photosynthesis, respiration, transpiration and light and rain interpretation (Zhu *et al.* 2018). Therefore, it has also importance in the estimation of carbon storage, thus it is a parameter used in different models: e.g., the absorbed active photosynthetic radiation, which defines the tree productivity, depends on LAI (Mäkelä *et al.,* 2008).

Traditionally, this parameter has been estimated using digital hemispherical photography, which consists of a camera and a wide lens pointing upwards taking photos. Recently, due to the improvement of satellite data it is possible to estimate it from satellite imagery. Now, drones are a third tool that can be used. Despite this, they are normally used to carry a camera to take photos or a laser equipment to create a point cloud of the canopy, and the drone is flown over it (e.g., *Khokthong et al.,* 2019 and Sumida *et al.,* 2009).

Over the last years, new techniques have been gaining importance among forestry professionals. New technologies, included in what can be presented as remote sensing, have increased its accuracy, and the scenarios in which they can be used have broaden.

One example for these innovative methodologies is the Unnamed Aerial Vehicles, commonly known as UASs. According to Banu *et al.* (2016), the first aerial photos were acquired in 1860 using air balloons, and it was not until 1950 that the first UASs were built. However, the use of this UASs was mainly for military missions. It was not until this last decade, that the use of UASs has been generalised for civilians. The first use of the UASs was basically in forest fires' monitoring (Ambrosia *et al.,* 2002 and Ollero *et al.*, 2006).

From that moment on, UASs use has been increased exponentially in forestry research. Despite this, it has been in the late years that relatively low-price UASs, with an easily portable design and with a hight quality camera integrated on them, that have been released. Two of the most known companies are Parrot and DJI.

Nevertheless, nowadays there is only one UAS that has the ability of taking photos upwards: The Parrot ANAFI. In this thesis it is going to be described a new method to characterize the forest canopy using this UAS model.

The aim of this document is to analyse the potential of the Parrot ANAFI by, using its integrated camera, fly the UAS throughout the canopy taking hemispherical photographs and test if this method improves or at least reproduces digital hemispherical photography.

1.2. Theoretical concepts

1.2.1. Leaf Area Index (LAI)

LAI is defined as one-sided leaf area per unit ground surface area (Chen and Black, 1992). In other words, is the amount of leaf area (m^2) in a canopy per unit of ground area (m^2) (Asner *et al.,* 2003). Different forms of analysis and methodologies of estimation exists, main classification being direct measurements or indirect estimations. LAI has become a central and basic descriptor of vegetation condition in a wide variety of studies.

However, as the form of canopy analysis vary, also varies the information extracted from it. One of the most used optical methods to derive LAI is digital hemispherical photography (Guangjian *et al.,* 2019).

Optical measurements normally work by quantifying gap fraction (probability of the sunlight penetration through the canopy) and in this way derive what is called the effective Leaf Area Index (LAI_e) (Ryu *et al.*, 2010). The fundamental equation that relates LAI with gap fraction is Beer-Lambert's law (eq. 1) (Nilson, 1971). The Beer-Lambert Law relates light absorption to the material properties, and it is widely used in calculating leaf area index and monitoring crop growing status (Tan *et al.,* 2020).

$$\ln\big(P(\theta)\big) = -G(\theta)LAI_e/\cos(\theta) \quad [1]$$

Where $P(\theta)$ is the gap fraction at the viewing zenith angle θ, $G(\theta)$ is the fraction of the leaf area projected on a plane normal to the zenith angle θ and LAI_e is the effective leaf area index. $G(\theta)/\cos(\theta)$ is the called extinction coefficient, or *k*, which is determined by the direction of incoming beams and the foliage inclination angle distribution (Zhu *et al.,* 2018).

Canopy gap fraction is defined as the probability of a ray of light passing through the canopy without encountering foliage or other plant elements (Danson *et al.,* 2007). Therefore, gap fraction is the degree of openness of the canopy: a bigger gap fraction is related to a higher level of light penetration. Most of the indirect methods to estimate LAI, use gap fraction. According to Cui *et al.* (2020), the vertical gap distribution can be used as an input to calculate the Vertical Foliage Profile with the Beer-Lambert Law, and then (as it is explained in the previous item) LAI can be estimated as an integration of LAD throughout the canopy.

Optical measurements can only derive effective LAI (Majasalmi, 2015), in contrast to true LAI, which is obtained after correcting this optical-derived effective LAI buy the woody area and clumping index (Majasalmi, 2005; Guangjian *et al.*, 2019). True LAI responds to next formula (eq. 2) (Guangjian *et al.*, 2019):

$$LAI = \frac{[(1-\alpha)\cdot LAI_e \cdot \gamma_E]}{\Omega_E} \quad [2]$$

Where α is the woody-to-total area ratio, γ_E is the needle-to-shoot area ratio and Ω_E is the element clumping index. This clumping index is a modifier of the LAI due to a non-randomly distributed canopy: i.e. conifer species with shooting-type growth (Majasalmi, 2015). This modifier is normally expressed as Ω. and can be expressed as the following equation (eq. 3) (Guangjijan *et al.,* 2019):

$$\Omega = \frac{\Omega_E}{\gamma_E} \quad [3]$$

Where Ω_E is the element clumping index at scales larger than the shoot and can be measured by optical instruments; and γ_E is the needle-to-shoot ratio that describes the clumping at smaller scales (shoot level). The latter must be estimated by destructive methods. In broadleaves forests $\gamma_E = 1$ and $\Omega_E = \Omega$. Therefore, clumping occurs at different scales (Chianucci and Cutini, 2012).

Normally, as clumping index is unknown, Ω is supposed to be one and methods call the resulting estimate effective LAI. Therefore, as it was previously said, optical methods will estimate LAI value that will include stems and area branches (Zhao *et al.,* 2011). Hence, this index estimation that takes into account woody and non-woody material and not corrected by the clumping index

is known as Plant Area Index (PAI) (Brüllhardt *et al.,* 2020). PAI is an estimate of the fraction of ground shaded by the vertical projection of tree crowns, and this parameter accounts for all the physical elements of the canopy (Sanusi *et al.,* 2017).

1.2.2. Leaf Area Density (LAD)

LAD, also known as foliage density, represents the area of leaves (m^2) per unit of canopy volume (m^3) (Weiss *et al.*, 2004; Jain *et al.,* 2010; Roberti *et al.,* 2019). LAD can normally be calculated at different heights of the canopy, and therefore the expression of LAD against canopy height is also known as foliage profile.

Nowadays, the main technique to estimate LAD is the use of laser technologies to count the number of leaves and their average surface in units of space known as voxels (volumetric pixels). Then, LAI can be estimated multiplying the LAD value by the height of each voxel (Jain *et al.,* 2010).

Therefore, it can be seen that LAI and LAD are somehow related. According to Cui *et al.* (2020), the total LAI requires the integration of the LAD from the canopy top to ground, as it can be seen in next equation (eq. 4).

$$LAI(h) = \int_0^H LAD(h)dh \qquad [4]$$

Where *H* is the total canopy height. Hence, the LAD values for different heights can vary throughout the whole canopy, but it is logical to think that the maximum LAI is obtained at the ground level. A study about leaf distribution in tree stands in Moravia (Èermák, 2014) shows how cumulative LAI gets its maximum at the bottom of the canopy.

There is also another parameter to be considered in the canopy description: foliage angle distribution. The foliage angle is the inclination of the foliage to the ground (Jain *et al.*, 2010). This parameter has to be taken into account when estimating other canopy parameters, as it affects the light environment that settles in the canopy, affecting the biophyisical interaction of sunlight and forest canopies (McNeil *et al.,* 2016). Depending on species, time, light… there are different foliage angle distributions.

1.2.3. Digital Hemispherical Photography

Digital Hemispherical Photography (DHP) is photographical technique used to calculate forest parameters, normally of a forest canopy. It is a well-established method to optically assess ecological parameters related to plant canopies (Glatthorn and Beckschäfer, 2014). It is based on a photographical equipment formed by a camera and a wide-angle lens pointing upwards in a completely flat position through the canopy to analyse the light environment and the leave characteristics. This system generally consists of a high-resolution digital camera, an extremely wide-angle fisheye lens, and a self-levelling system to ensure that it is held horizontally (Guangjian *et al.*, 2019).

The image taken, composed by a three RGB bands, is used afterwards to estimate the gap fraction. This is normally conducted by setting a threshold to classify each pixel in either plant material or sky. A software will after that determine if each pixel is or not plant, resulting in a binary image from which can be deduced the gap fraction and then LAI.

The use of DHP is flexible but brings perceived sensitivity of the results to several factors, including photographic exposure, gamma function and classification threshold (Guangjian *et al.*, 2019). To make this classification, it is usually used the blue band value, as the contrast between

sky and vegetation is higher in the region of the blue (Chianucci and Cutini, 2012; Glatthorn and Beckschäfer, 2014).

There are three main effects that have to be beard in mind while classifying grey pixels in a software of these characteristics (Glatthorn and Beckschäfer, 2014):

- **Position of the pixel within the photograph**: as the illumination changes across the different sections of a photograph, pixels close to the zenith are brighter than pixels close to the horizon.
- **Blooming effect**: this effect means that the saturated sky pixels may influence the gray value of neighboring vegetation pixels.
- **Reflection at vegetation**: it is possible that the angle of incidence of sunlight affects the gray value of the rest of vegetation.

Moreover, as introduced before, there are also some more parameters that affect the final value of LAI in digital hemispherical photo processing.

First of all, the wood-to-non-wood area ratio α, represents the relationship between wood material (such as stems or branches and leaves). This elements intercept radiation before it reaches the forest floor and affect optical measurements made near the ground. This parameter is invariant with the season (in conifer boreal forests) and it has to be determined once by destructive methods (Chen, 1996). Other computational methods such as machine learning with training and testing photographs can be studied too. If this aspect is no taken into consideration, the final LAI is overestimated.

Secondly, the clumping effect, what is a consequence of non-randomly distributed leaves. As treated before, there are two levels of clumping (Weiss *et al.,* 2004; Chen *et al.,* 2006; Chianucci and Cutini, 2012 Majasalmi, 2015):

- Clumping at a shoot level (within-shoot level), what is characteristic of needle-trees such as pine or spruce, but not of broadleaves. This level is related to the forms that the needles distribute in the shoot, unifying themselves according to pre-established growth patterns. This level is described by the needle-to-shoot ratio γ_E, which is a relation between the area of the needles in a shoot and the shoot area (Chen *et al.,* 2006).
- Clumping at a canopy level (beyond-shoot level), which is related to the gap size distribution. Canopy gap size distribution characterizes the spatial variability of canopy transmittance at different hierarchical levels. This level is described by the element clumping index Ω_E , that quantifies clumping effects at scales largher that the shoot level (Ryu *et al.,* 2010).

Therefore, this clumping index Ω is a dispersion parameter that is determined by the spatial distribution pattern of leaves. If the distribution is random, it is unity and does not affect the sunlight transmittance of the canopy; but if leaves are more clumped, then the index negatively affects the radiation interception (Chen *et al.,* 2005).

Clumping is a parameter that can be derived optically from optical measurements of effective LAI: the accurate estimation of effective LAI will help to constrain Ω as well (Ryu *et al.,* 2010). However, there are also various computational methods of clumping index estimation (Gonsamo and Pellikka, 2009). The problem with clumping effect and LAI is that normally

software that estimate LAI leads to a underestimation of LAI if a simple random-distribution model is used in a place that clumping index is different from 1 (Gonsamo and Pellikka, 2009).

Finally, there is another issue that leads to an underestimation of LAI and that is related to the previous one: the overlap of leaves. Overlapping is, with clumping, the two main problems that cause underestimation of LAI (Zheng and Moskal, 2009). The level of overlapping depends on the canopy architecture and species structuration. Overlapping of leaves make that looking upwards, some leaves are hidden behind other ones, and therefore the optical-estimated LAI is underestimated.

1.2.4. Unmanned Aircraft System

According to EU Regulations 2019/945 and 2019/947 of European Commission, a Unmanned Aircraft System (UAS) is a unmanned aircraft and the equipment to control it remotely. Unmanned aircraft means any aircraft operating or designed to operate autonomously or to be piloted remotely without a pilot on board. An UAS has three components: an autonomous or human-operated control system which usually on the ground or a ship but may be on another airborne platform; an Unmanned Aerial Vehicle (UAV) and a command-and-control system to link the two.

In this thesis, UAS will reference two the Remotely Piloted Air System (RPAS) which will be used to estimate forest parameters. Please note that in the data-collection, all the safety regulations have been followed, as well as the geographical restrictions.

Nowadays, UAS are increasingly being used in estimation of forest parameters. UAS are being used to estimate light environmental conditions, normally as a platform to use other techniques such as DHP, laser scanning, multispectral imagery… Some examples of this boost are the work of McNeil *et al.* (2016), where they compared UAS-based measurements of leave angle against those made from conventional levelled digital photographs taken from towers, ladders, buildings or poles; the work of Brüllhardt *et al.,* (2020) where they used UASs to estimate light transmissivity throughout the canopy and were able to study vertical light profiles in forests; or the work of Krisanski *et al.* (2020), where they used UAS-based photogrammetry to study forest parameters such as stem diameters.

There are very few references of UAS-based hemispherical photography. Normally, UASs are used to carry laser scans or normal cameras rather than equipment with capacity to take hemispherical photos. Therefore, UASs are used either as an airborne laser scan methodology or as an optical methodology (to take single or multiple photos, to which apply photogrammetry techniques). There are lots of examples of these procedures (McNeil *et al.*, 2015; Agus *et al.*, 2018; Abdollahnejad *et al.*, 2018; Krisanksi *et al.*, 2020; Agus and Danoedoro, 2021). In all the cases, the drones used have to be big enough to carry that equipment.

Moreover, UAS-based photos are normally taken downwards. Brawn *et al.* (2020), designed a methodology to compare digital hemispherical photography traditionally taken (SLR Camera and Fisheye lens) to UAS-based hemispherical photography. In that case, they studied an agricultural crop, and therefore both methodologies were compared taking photos downwards.

The aim of that work was to estimate the crop's LAI and compare both methods. They used a 3DR drone equipped with a GoPro HERO4 pointed downwards. Their results showed that both methodologies were equally accurate. A similar method was used in the work of Uribe *et al.* (2018).

1.2.5. Spherical photos

Spherical photos are images that capture all the field of view surrounding one point in space. This photographical technique is used to represent the 360-degree right/left and the 180-degree up/down field of view.

Since the technology required was released, spherical imagery has been used specially for virtual reality. Virtual reality (VR) applications became increasingly popular, and the demand for image processing methods raised (Ruder *et al.*, 2018).

However, recently, this spherical imagery has started also to have a use in forestry. Works about forest parameter estimation have based in spherical photos have increased in last years. Examples of this are the work of Itakura and Hosoy (2020), that worked on automatic tree detection from three-dimensional images based in 360-imagery; the work of Wang *et al.* (2021a and 2021b), about estimation individual tree heights, diameter at breast height and basal area; or even the use of smartphone-based spherical images to estimate forest light environment and canopy structure (Andis Arieta, 2020).

1.3. Objectives

1.3.1. Method development and validation

The first aim of this thesis is to test how close are the results of LAI both estimated using traditional digital hemispherical photography (i.e., single-lens reflex camera and wide-lens) and hemispherical photography captured with a UAS, in this case the Parrot ANAFI.

1.3.2. Vertical canopy profiles

The second objective of this thesis is to study the potential of flying this Parrot ANAFI throughout all the canopy in order to acquire information at any height, and therefore be able to construct a vertical profile of the canopy using only optical techniques. A review of this potential will be done.

2. MATERIALS AND METHODS

2.1. Materials

2.1.1. UAS: Parrot ANAFI

The 1st of July of 2018, the French enterprise Parrot launched the Parrot ANAFI (Parrot Drones SAS, Paris, France). This drone was characterized by having a hight quality camera and by its ability of looking upwards thanks to its 180° tilt gimbal. Thanks to that, this drone has the ability of taking spherical photos. These characteristics, in addition to a very affordable price for a drone of its capacities (around 700 €), make it the target of this thesis in order to describe its potential in forest applications.

Next, some more technical specifications of this UAS can be found.

UAS

- Size unfolded: 175x240x65 mm
- Weight: 320 g
- Max flight time (one battery): 25 min
- Operating temperature range: -10° C to 40°C
- Satellite Positioning Systems: GPS and GLONASS

Imaging system

- Sensor: 1/2.4'' CMOS
- Lens
    - ASPH (Sharper images)
    - Aperture: f/2.4
    - Focal length (35 mm format equivalent)
- Shutter speed: electronic shutter 1 to 1/10000 s
- ISO range: 100 – 3200
- Photo resolution
    - Wide: 21MP (5344x4016) / 4:3 / 84° HFOV
    - Rectilinear: 16MP (4608x3456) / 4:3 / 75.5° HFOV
- Photo formats: JPEG, DNG (RAW)

Image stabilization

- Stabilization:
    - 3-axis hybrid
        - Mechanical: 2-axis Roll/Tilt angles
        - Electronic (EIS): 3-axis Roll/Pan/Tilt angles
    - Controllable tilt range: - 90° to +90° (180° total)

2.1.2. Digital hemispherical equipment

The traditional digital hemispherical photography equipment used is composed by a single-lens reflex camera and a fisheye lens, mounted in a specific tripod and gimbal to be able to point the equipment upwards. These elements, which are going to be briefly described next, are: camera Canon EOS 70D (average price 1,000 €), lens Sigma 4.5 mm (average price 1,000 €), self-levelling mount type SLM9 AT Delta-T Devices Ltd (average price 2,000 €) and a tripod (average price 250 €).

Canon EOS 70D

The main physical specifications are its operating environment, 0 – 40 °C and maximum of 85% air humidity, and its weigh and dimensions: 755 g and 139.0 x 104.3 x 78.5 mm, respectively.

This camera has a 22.5 x 15.0 mm CMOS sensor, with 20.2 megapixels. The shutter is electronically controlled and focal-plane shutter, with a speed of 30-1/8000 sec. ISO sensitivity ranges from 100 to 12800 and can be expanded to H: 25600. Shooting formats are JPEG, DPOF and RAW. Image size used, despite varying in different ranges, is 1:1 3648x3648.

Sigma 4.5 mm F2.8 EX DC Circular Fisheye HSM

With a weight of 470 g and dimensions (Diameter x Length) of 76.2 x 77.8 mm, this lens is specifically designed to take wide-angle photos: the angle of view is 180° (90° from the zenith to each side). The focal length can vary from 17 to 55 mm and the aperture can vary from F2.2 to F2.8. The maximum magnifications are 1:6. This lens also incorporates an optical stabilizer to compensate for camera shake and it is equipped with a hypersonic motor to optimize autofocusing and quiet operation.

Self-levelling mount type SLM9, AT Delta-T Devices Ltd

This self-levelling mount is intended for the use with either a tripod or a monopod. It helps keep a camera and fisheye lens aligned to the horizon and North. This is specifically designed for taking hemispherical photos. It has an approximate weight of 1 kg.

This device is equipped with two mechanical gimbals to align each axis N-S and W-E to be completely flat. Each gimbal is equipped with adjustable levelling weights and the inner one eith a bubble level to adjust the weights. It also has a compass, which allows to align the camera with the North. Moreover, there are two marks (each for North and South) in the inner gimbal, that can be seen after taking a photo, and this way it can be known the South and the North in the hemispherical images.

2.1.3. Software

2.1.3.1. Hemisfer 3.1

Hemisfer is a commercial software designed by WLS Swiss Federal Institute for Forest, Snow and Landscape research. It is used to process hemispherical photos analyzing the image and extracting information such as LAI and light environmental characteristics.

Basically, this program classifies each pixel of the image into vegetation or sky. This classification can be automatic and manual or prefixed (Chiannucci and Cutini, 2021), and it is based in a threshold calculation that classifies each pixel attending to its RGB value. Hemisfer presents two methods of automatic calculation: Nobis & Hunziker (2005) and Ridler & Calvard (1978). According to the user's manual, the first method requires the analysis of many pixel to establish the ideal value for the threshold, and despite taking for that reason a bit more time for the classification, it normally gives better results than the other one. The way the program works is to transform the image in a grey-tones image, and then using that threshold, it is converted into a black and white image. Then, the black pixels (vegetation) are counted against the white pixels (sky).

The first main output of this program is Leaf Area Index (LAI). This software has six different ways of calculating LAI, and four different corrections. Therefore, in the output data file, it can be seen all the different values according to each methodology applied, though it does not result in a very high difference among them. The software cuts the image in sectors from its center and analyzes separately each of them. As this software operates with the generation of a threshold, the LAI output value is the effective LAI, as there is no discrimination in woody or leaf material. However, one of the corrections, does adjust the effective LAI with the self-calculated clumping index. In this thesis, as the aim was to qualitatively compare traditional DHP with UAS-based DHP, a mean of the minimum and maximum values was the LAI value assigned.

A manual adjustment of the threshold in order to minimize its negative effect can be done if it is observed that the transformation is not done with enough accuracy.

Other parameters obtained when running an image in the program are the openness and the total gap fraction of the image, the clumping index for each sector and, depending on the method used, the leaf angle.

However, the other main output is a data file in which the light regime is described. What can be extracted for that file is the potential and effective diffuse or direct radiation on a horizontal and inclined surface for each day of the period established. Therefore, it can be known the

radiation that affects the canopy shown in each hemispherical image. Furthermore, the file gives the diffuse, direct and global light index for the site and the period established.

Inputs required for this program are lens characteristics (field of view and deformation parameters) and colour settings for threshold calculation (in this adjustment can be settled the preference for blue band against the green and red, for example) for LAI estimation and site coordinates and period of the year for light environment results.

2.1.3.2. Parrot ANAFI software

FreeFlight 6 App (version 6.7.1) developed by Parrot was used to control the UAV. This app not only allows to control the UAS, but also to deal with all the photos taken.

When spherical or 360 photos are taken, the UAS stabilizes itself in flight and starts taking photos all around him. The UAS will take 42 photos covering a sphere with center in the UAS. These photos will be kept in the SD card.

Afterwards, in the FreeFlight 6 App, these photos can be accessed and the order of constructing the spherical image can be given to it (figure 1). Therefore, it is the Parrot inner software itself the one which is used to create a spherical image using all the images taken around him. The next step can be downloading this image to the phone and then passing it to the computer.

Fig. 1: Spherical image taken at 5 m from the ground in the middle of a 25m-canopy. It can be seen the big distortions both at bottom and top of the image.

Other useful information that can be extracted from the FreeFlight 6 Parrot app is, for every flight, a data file containing flight timing, GPS positioning and compass information, which can be either directly consulted or downloaded.

2.1.3.3. Other used software

Despite previous programs are the main used software, it has been also used Python script written by Haozhou Wang (2019) and posted in GitHub web page (https://github.com/HowcanoeWang/Spherical2TreeAttributes), which allows to transform a spherical photo into a hemispherical one. In this thesis, it will be used to transform the spherical images built by the Parrot ANAFI software. Other programs have been punctually used, such as GIMP 2.10.22, Image Magick , ShowAnafiLog and Microsoft Image Composite Editor 1.4.4.0. Its use will be explained in methods.

2.2. Methods

2.2.1. Method development and validation

The procedure followed in the method development and validation testing is shown in figure 2. Next sections will go through the procedure.

Fig. 2: Flow path of the new methodology presented. [Source: own elaboration.]

First step was to identify the places in which take photos with both equipment. Due to logistical reasons, the first data collecting took place in the green areas that surround the Pihjalamaki University of Helsinki Housing, Viikki, Helsinki. Five points were selected in the Vuolukiventie surroundings, seven points in the Viikki University of Helsinki Arboretum (figure 3) and 10 more points at the Hakalanniemi zone of the Viikki UH Arboretum (figure 4).

Fig. 3: Location of the 11 points of the testing. Left, Vuolokiventie; right Viikkin Kampus University of Helsinki Arboretum. [Source: own elaboration using Google Maps].

After arriving to each point, and after validating it, the scenario was prepared to take the photos. Timing for each methodology was controlled. After disposing the tripod and the self-leveling mount and leveled to face exactly the vertical using an integrated bubble-level, the camera was connected via wi-fi to the mobile phone. Camera was pointed north with a magnetic compass.

Fig. 4: Location of 10 points of the testing at the surroundings of Hakalanniemi natural area. [Source: own elaboration using Google Maps.]

Vuolokiventie's photos were taken in a Scots pine stand (*Pinus sylvestris* L.) of about 700 trees/ha and a canopy height around 10 meters. Viikkin Kampus and Hakalanniemi photos were taken in the UH Arboretum spruce (*Picea* sp.) stands, with an approximate tree density of 1,500 trees/ha and a canopy height of 20 meters. These differences were sought in order to achieve enough LAI variation, to stratify this method development and validation sampling.

In order to standardize the procedure, a protocol was designed to adjust the camera parameters. The exposure is one of the most important issues in DHP (Chianucci and Cutini, 2012; Beckshäfer *et al.*, 2013), as it defines the over or underestimation of LAI. Thus, it was partly followed a standard protocol for hemispherical photographs (Glatthorn and Beckschäfer, 2014).

As it has been said, one of the most important aspects of DHP is exposure, and to avoid overexposure (and therefore underestimation of LAI) it is crucial to previously adjust the parameters that affect that variable: time of exposure, ISO and openness of the sensor.

ISO is normally set up at 200, as it is recommended not to increase it very much, and always below 400. To adjust the other two parameters, it was followed that protocol, which establishes that the exposure must be set up according to the brightest part of the photo. Therefore, the procedure was as next:

- Taking a photo in auto-exposure mode.
- Evaluation of the RGB and grey histograms in the camera.
- Manually adjustment of the exposition and openness until the grey histogram did not show overexposed pixels (in other words, until the grey histogram did not show a peak in the right part).

Apart from that, always days of diffuse light rather than completely clear ones were chosen to collect data.

After that, the camera equipment was disassembled and stored. Next step was preparing the UAS. First thing to do was set up the taking off and landing surface in the exact point that the tripod of the camera had previously been. After, the UAS had to be calibrated (only the first time) and then it could take off and start taking the spherical photo.

To take this spherical photo, the UAS started a steady flight at the height and location wanted, and then started taking photos. In this case, the flight location was the same of where the tripod had been before, and the height of flight was the same approximately to the height of the camera set onto the tripod, so 1 meter from the ground.

The whole process of taking a spherical image is summarized below:

- Take off with the camera facing randomly (it is important to bear this in mind in order to know the deviation from north that will be addressed later).
- Wait to have enough GPS signal and stabilize the UAS at 0 meters from the take off point and at a height of 1 meter.
- Begin the spherical image. This process involved taking four photos per each azimuth or visual direction of the UAS, and one upwards and downwards. After the four photos per visual, the UAS rotated approximately 36 degrees and took next group photos.
- Once the UAS visual had given a whole spin, it stopped in the same visual that started.

This process took about 2 minutes per photo. After that, the UAS was landed in the landing surface and stored. In next point, the procedure was repeated.

2.2.1.1. Photo processing

SLDR Camera

Photos from the Canon and Sigma equipment were download into the computer. In this primary testing, the format of the photos was .jpeg. In case they needed some editing (Windows 10 Photo Editor), for example for adjusting the light level to a more similar display than the UAS, it was done in this phase. Photos were 3648x3648 pixels and of a resolution of 72x72 ppp (pixels per inch). The name for each photo was codified attending to the date and the point in which it had been taken.

Parrot ANAFI

After taking the photos, the FreeFlight 6 App was used to transform the 42 photos the UAS had taken into a spherical image. The way this software works (Parrot ANAFI user's manual, 2018) is by downloading the photos in the smartphone, stitching them using the common surface among the photos, and then creating the panorama. This panorama image can be looked at in the FreeFlight 6 gallery in a Virtual Reality mode or exported to the smartphone in the equirectangular projection. Afterwards, it was downloaded into the computer. This image was also named attending to the date, point and with the categorization of "Sphere". These spherical images were 8000x4000 pixels and the same resolution than the canon ones. They also were .jpeg format too (figure 5).

However, in some cases the software Microsoft Image Composition Editor was used due to problems in the FreeFlight 6 App. In those cases, the procedure was to download the 42 images from the SD card of the UAS directly into de computer, and then process these images in the software.

The inputs required for this software were the original individual images (in this case, the 42 images for each spherical image). This program requires to be told what type of camera motion

had the device that took the photos. In this case it was set to automatic so that the software itself filled this information accordingly to the input photos. Therefore, the camera motion was set to "Rotation Motion", which is logical according to the procedure the UAS takes in each spherical photo (see above). After this spherical image was built, photo settings were modified in order to make them coincide with the images exported with the FreeFlight 6 App. These adjustments were:

- Photo width: 8,000 px
- Photo height: 4,000 px
- Photo resolution: 72 ppp

Fig. 5: Hemispherical photo transformed from the spherical one at figure 1.

The spherical image was created with equirectangular projection, one of the most common projections for spherical imagery. (Ruder *et al.,* 2018). In this projection, the distortion becomes very large on the poles of the sphere. Then, this spherical image had to be transformed into a hemispherical one, with polar projection (figure 5). In this step of the thesis development, was directly used a script developed specially to transform spherical images into hemispherical (Hang, W., 2019), and the script was roughly run to convert the images. However, it will probably be developed a software tool to integrate this step in the further ones.

These hemispherical images were 4000x4000 pixels and a resolution of 96 ppp. This increase of the resolution is logical, as from the upper 21 photos of the upper part of the sphere, it is created one single image. These images were again codified by date, point and the category "fisheye". Next step in the methodology was to process the images in the Hemisfer software. First, the Hemisfer parameters were adjusted as it is shown in the following:

- Lens:
  - For DHP it was used a Sigma 4.5 mm and a field of view of 75°.
  - For UAS it was used as a linear lens, as it was considered that the hemispherical photo built by the script had no distortion. Field of view of 90°.
- Colour: this parameter affects the band (from the RGB bands) most used to calculate the threshold. It was set to by default at 33R, 33G and 34B. In case of problems at the threshold calculation, more importance was done to the blue band.
- Threshold: the Nobis and Hunziker (2005) method was used to calculate the threshold. The parameter gamma, which according to the Hemisfer user manual indicates how the color coding in the picture relates to the physical light intensity, was set to 2.2 by default.
- LAI parameters: all the methods were marked to be calculated, as well as the corrections available. Other parameters such as leaf angle were set in de default values.

In the results, as there where over 25 values of LAI (due to the diverse methodologies and the corrections applied), the maximum and the minimum values were used to calculate an average, average that was considered the final LAI value of each photo. In this document, LAI estimated is effective LAI or Plant Area Index (PAI), as it has not been corrected by clumping index nor woody/non-woody ratio (Chianucci and Cutini, 2012).

2.2.1.2. Metadata reading

Apart from analyzing the LAI of each photo, metadata was used to know how the UAS was working when taking the photos. To check this metadata, it was used the software ImageMagick and a self-coded script. What was wanted to know was the orientation of the final hemispherical photo from north. This was not important for LAI but for light environment condition, and as the further aim was to develop a tool to estimate light environment and incident PAR, it was set as an objective to discover the rotation of the photos.

Therefore, metadata was read from the spherical image, the final hemispherical image and the first of the 42 photos taken by the UAS when starting the spherical image composition in field. From those metadata, a camera and a UAS yaw angle were found in the latter photo. Those angles where the ones compared to the manually extracted angle of rotation from north. This angle was extracted in a photo editor (in this case, GIMP) observing the rotation needed in comparison to the DHC photo from the same spot, which was oriented to magnetic north. This metadata comparison was done only for ten photos (P0 – P4 and P6 – P11).

2.2.1.3. Statistical analysis

The statistics used in this primary testing is basically linear regression to study the correlation between the two methodologies of LAI estimation. Hence, the basic parameters to study the correlation between them is the coefficient of determination (R^2) and the linear equation (eq. 5):

$$LAI_{DHP} = aLAI_{UAV} + b + \varepsilon \quad [5]$$

In which LAI_{DHP} is the LAI obtained by the Canon and Sigma equipment, LAI_{UAV} is the LAI obtained by the Parrot ANAFI, a and b are the linear equation parameters and ε is the error

between estimations. Ideally, the a parameter should be the unit and the b parameter should be zero, this way the error should be zero and the coefficient of determination would be the unit. The more these parameters are close to those ideal values, the better correlation between both methods.

To compare both methods, it has also been studied the bias between both methods, considering the real estimation of LAI the one derived from traditional digital hemispherical photography. Hence, bias is estimated as $LAI_{UAV} - LAI_{DHP}$.

2.2.2. Vertical canopy profiles

First requirement was to identify the ideal spots for a vertical profile analysis of the canopy. This meant places that had a clean vertical that allowed the UAS to ascend without any problem (limitations of this part will be presented at the discussion).

After identifying the ideal locations, the UAS took off and started taking the spherical images at different heights. The more photos taken in a same ascension, the more points of information would be available for the further description of the canopy. In this thesis it was decided to take photos of the canopy each 2 meters, as the caption of the variation each 2 meters was supposed to be enough sensitivity to study the LAI and the LAD variation with height.

As the UAS has a minimum height flight set to 0.5 meters, first photo was taken at that height but was categorized as 0-meter photo. Next photos were taken after the height sensor marked 2-meter ascension. In case that it was needed, the log files of the flight could be checked. This 0.5-meter height deviation is considered to be assumable, as the LAI variation in 0.5 meters is insignificant.

After, images were processed and analysed in Hemisfer. As the definition of LAI is the integral of LAD throughout the canopy height, this relation can be used the other way around to calculate the LAD between different height layers. In this document, next formula was used (eq. 6):

$$LAD_{ij} = \frac{LAI_i - LAI_j}{h_j - h_i} \quad [6]$$

Being *i* the first layer (lower height) and *j* the second layer (upper height) and *h* height.

3. RESULTS

3.1. Method development and validation

3.1.1. Methodology comparison and accuracy

When both methodologies were compared (so LAI estimated by traditional digital hemispherical equipment and the Parrot ANAFI UAS), it was seen that there was a good correlation. The coefficient of determination was high (R^2 = 0.7963) and the deviation from the 1:1 line had a very reasonable value, despite the fact that there was a deviation of 0.4 (figure 6).

In the first place, assuming that the LAI measured with the traditional digital hemispherical equipment is the value that is considered the real one (statement that will be treated further on) it can be derived from figure 6 that specially in high values of LAI, the UAS-estimated LAI is underestimated. The bias can be seen in figure 7.

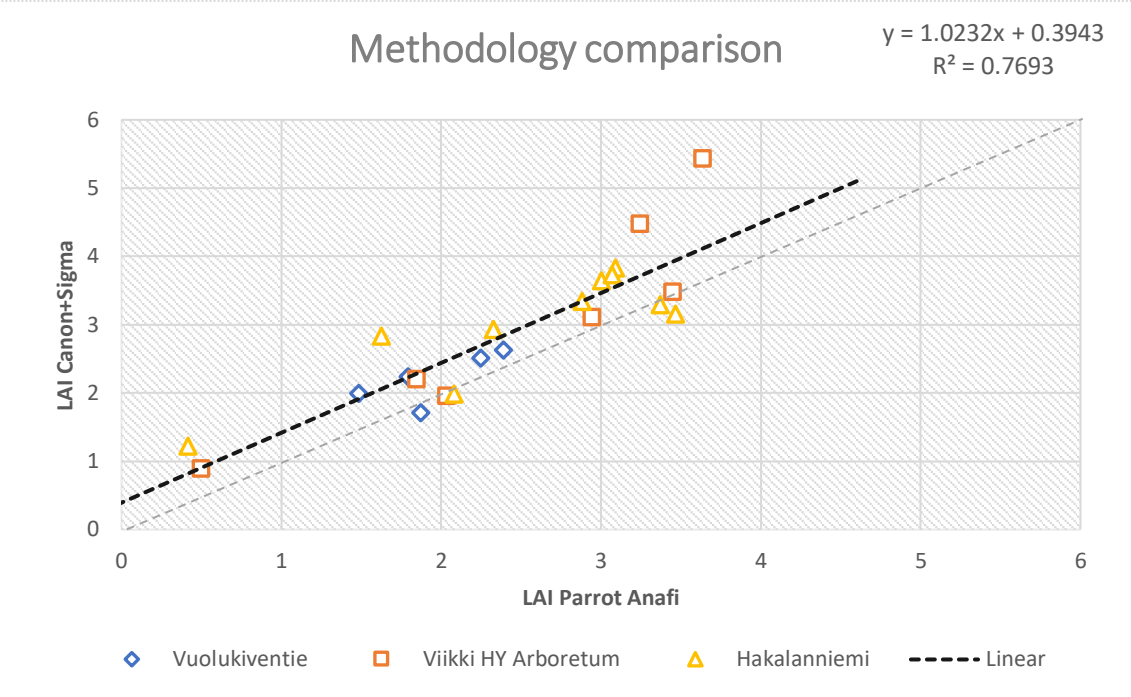

Fig. 6: Comparison of both methodologies studied. In blue, data from Vuolukiventie; in orange, data from Viikki HY Arboretum and in yellow, data from Hakalanniemi. LAI in m^2/m^2. [Source: own elaboration].

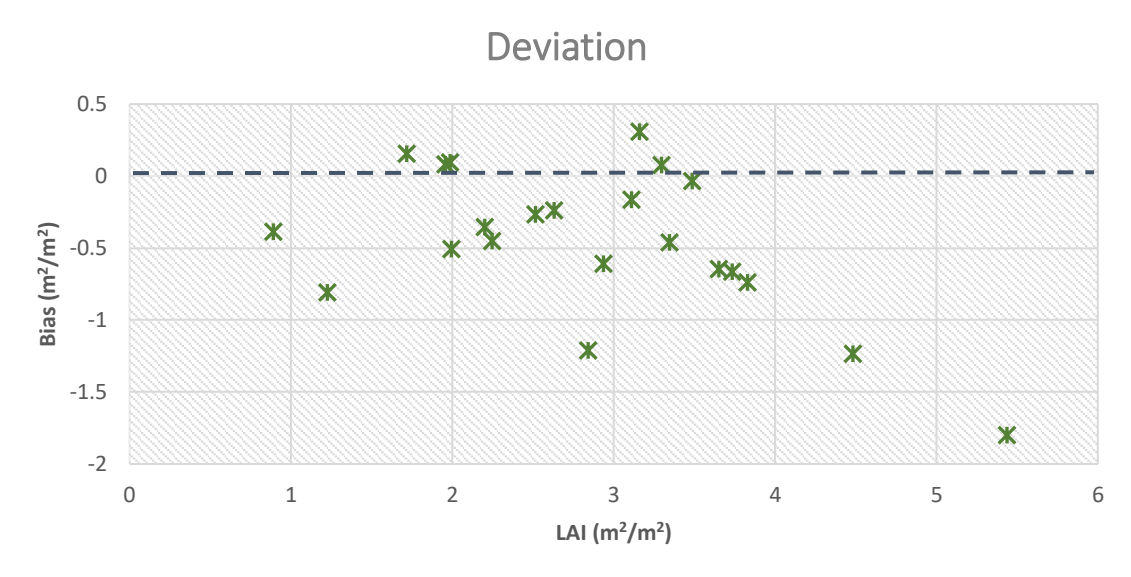

Fig. 7: Bias between LAI (DHC) and LAI (UAS). Deviation is calculated as the latter minus the first one. [Source: own elaboration.]

The mean relative value of bias in relation to the LAI (DHC) is an underestimation of 16.4%, calculated as the deviation in relation to the DHC LAI value. In figure 8 it can be seen that the most biased sample points are 6, 7, 11, 17 and 21.

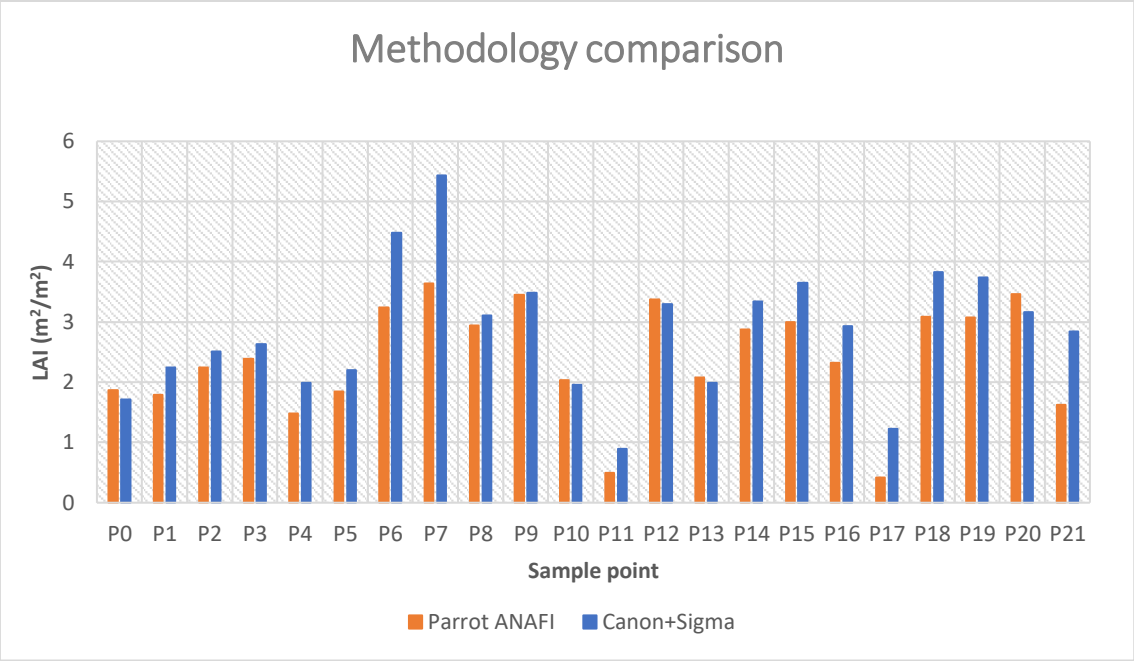

Fig. 8: Differences in LAI between Parrot Anafi and Canon camera and Sigma lens. [Source: own elaboration].

Nevertheless, after analysing the differences between hemispherical photos from different points, a possible explanation has been found for that underestimation. If both DHC and UAS photos are inspected, it can be seen that the image resolution might have something to do with this underestimation. Figure 9 show the quality difference between photos of each methodology.

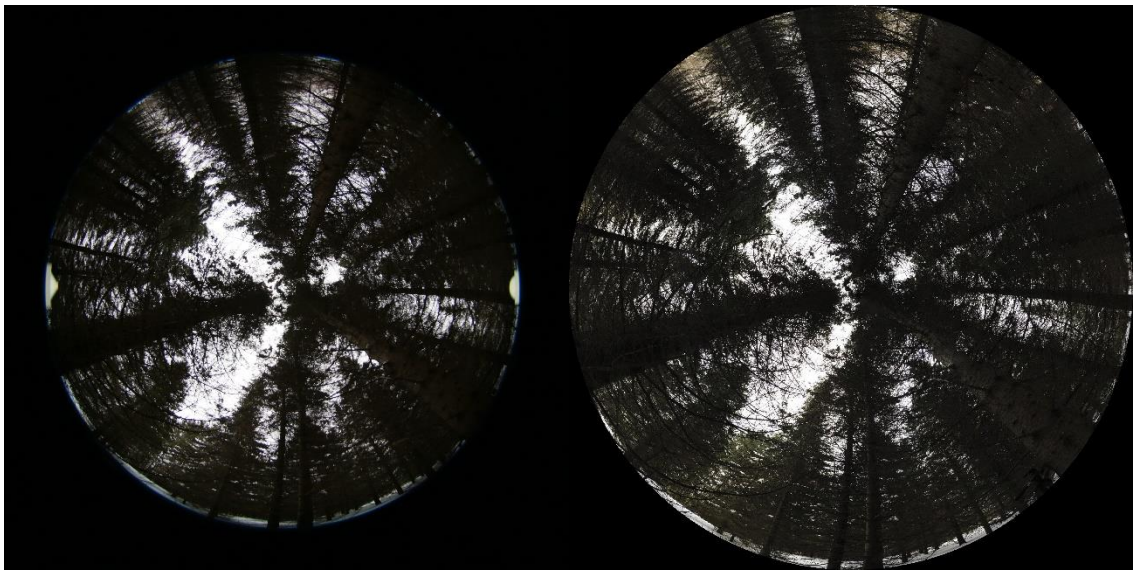

Fig. 9: Hemispherical images from DHC (left) and UAS (right).

As it can be seen, the image quality is much better in the hemispherical image taken with the UAS. This is a very logical observation, as the UAS-based hemispherical image is a result of the combination of 21 photos of 21 megapixels each, while DHC-based one is the result of a single photo of 20.2 MP. Figure 10 shows a detail of this difference in resolution.

Fig. 10: Detail of the previous photos. Resolution is lower in DHC-based image (left) than in UAS-based one (right).

As it has been explained before, to derive LAI, Hemisfer software first calculates the gap fraction. To calculate gap fraction, it sets a threshold automatically, and uses that threshold to characterize each pixel into vegetation or sky. The more quality the image the image has (speaking of resolution), the more precisely the image will be classified, and therefore a more accurate value of LAI will be derived. Normally, the more vegetation there is (and especially when this vegetation is very intertwined) the more pixels that are misunderstood.

To quantify this, a sub-section of the picture above was cut and converted into a black and white image using Hemisfer to be able to derive gap fraction. This section was established in the center of the image, in the central annulus of the Hemisfer projection, so that the gap fraction could be considered constant in that ring (the same Hemisfer does). The images can be seen in figure 11.

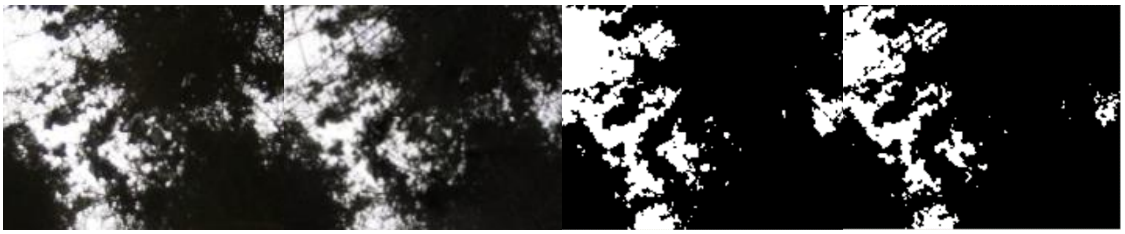

Fig. 11: Comparison of the details: left coloured (1) DHC; (2) UAS; and right black and white: (3) DHC; (4) UAS. [Source: own elaboration.]

By calculating the percentage of white pixels in relation to the total pixels of the images, the gap fraction has a value of 18.5% in the DHC photo and 12.2% in the Parrot ANAFI photo. These values are consistent with the gap fraction derived by Hemisfer in the center of the image. If the gap fraction calculated by the software is analysed, the annulus 1 and 2 (so the zenith of the hemispherical photo) are the only ones that have a bigger gap fraction in the DHC photo, whereas in 3 to 5 annulus (the biggest ones) the gap fraction is less in DHC photo. As the global gap fraction (and thus the total LAI) is weighted by the surface of the annulus (i.e. number of pixels), the global value of gap fraction is lower in DHC photos than in UAS photos, and consequently, the LAI is bigger in DH photography. In fact, if the whole images are converted to black and white and analysed the white/total pixel relation, gap fraction is again lower in DHC photo, and consequently LAI is bigger. To summarize, there are clear differences in resolution, but these differences are subjected to another factor: the projection of the image (i.e. the annulus of Hemisfer).

Moreover, after the hemispherical images were created, it was qualitatively treated the stitching error by analysing a subsample of the photos. Figure 12 shows some errors located.

Fig. 12: Examples of stitching errors located. [Source: own elaboration.]

3.1.2. Other results

3.1.2.1. Timing

When taking each photo, the time inverted in each methodology was measured. The results show that the UAS-based method is much faster than the DHC one (figure 13). This is because the UAS was very easy-portable and very easy to prepare.

The preparation of the DHC required preparing the tripod, the self-levelling mount, the camera, the lens and the north orientation. Then the wi-fi connection to the phone to remote control the camera, and finally the exposure parameter adjustment. On the other side, the Parrot ANAFI only required to be taken out from its case, turn it on and connect to the remote controller and the phone, which was faster. Then the 360-image taking itself, which lasted about 2 minutes.

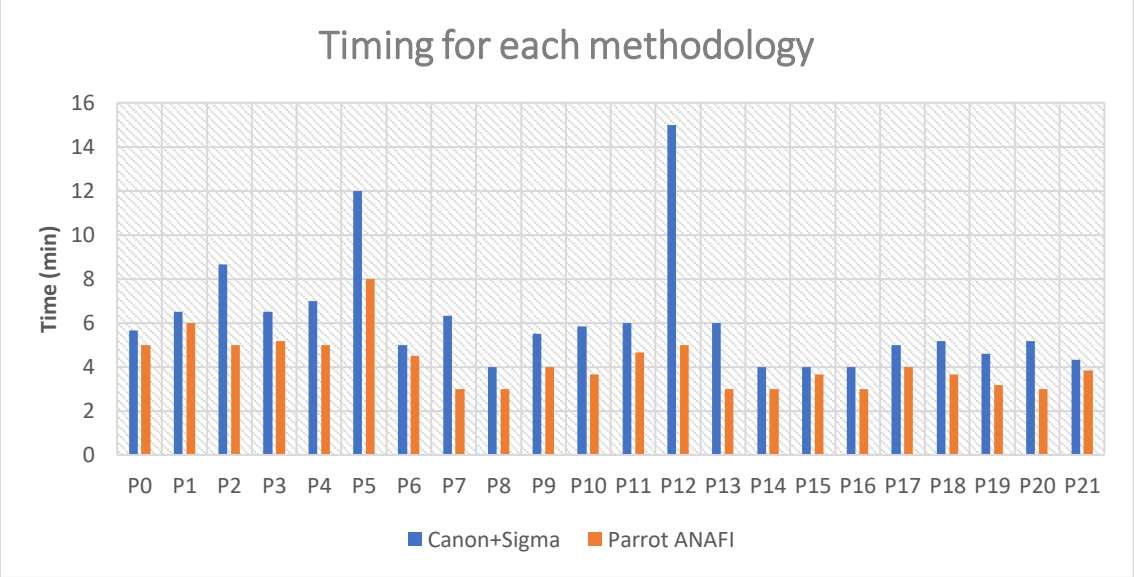

Fig. 13: Timing comparison for each methodology. [Source: own elaboration.]

Please note that figure 13 only shows illustrative values, as the timing for each photo is dependent on other aspects relative to personal disposure of the photo manager.

However, it must be said that despite the Parrot ANAFI was faster in the field, the processing of the images was easier in the Canon+Sigma photos. This is because the Canon+Sigma photos could be directly downloaded into the computer and directly processed in Hemisfer, whereas

the 42 raw photos taken by the UAS had to be compelled into the spherical image (either on the FreeFlight 6 App and then download the spherical image or downloading the raw photos into the computer and introduce them in the Microsoft Image Composition Editor to build the spherical image), and then transformed into hemispherical image using Python. Only then, UAS photos could be processed in Hemisfer.

3.1.2.2. Angle verification

As it was explained before, in order to understand the inner functioning of the Parrot ANAFI, the metadata of the photos was analysed. The aim of this was to know the rotation angle form north that had each of the hemispherical photos taken.

Despite the azimuth (so the north orientation angle) is not needed for the LAI estimation using hemispherical photos, it is required to study other parameters, such as light environment.

Therefore, 10 photos were selected and metadata from first raw image was read to know the north orientation of the UAS. Also, these photos were rotated in an image editor and compared with the DHC images (where the north was known) to see the actual rotation of the UAS images from north. Afterwards, these two angle values were plotted (figure 14).

Main result was that metadata from the first raw image indeed indicated the azimuth of the UAS, but it was also observed that there was a deviation that was repeated in each photo. Comparing the actual rotation (so the angle extracted comparing DHC and UAS photos in the image editor) and the angle identified in the first photo metadata, it was identified an error that ranged from 0.5 to 60 degrees. However, the majority had an error value much closer to the average of 20 degrees.

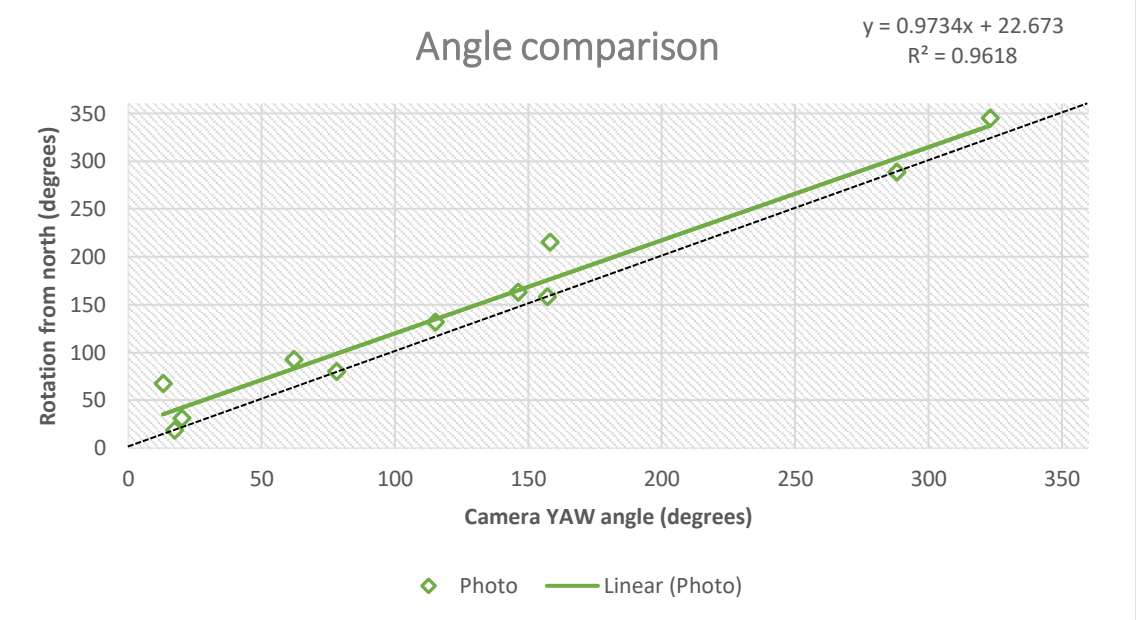

Fig. 14: Comparison of the angle extracted from first raw photo metadata and actual rotation from north extracted in the image editor. [Source: own elaboration.]

Figure 14 shows that the deviation of 20° is very constant. If the regression parameters are analysed, the correlation coefficient is very high ($R^2 = 0.9581$) and the deviation from the 1:1 line is practically null. Therefore, it can be stated than the north angle error is not dependant on the azimuth value. This azimuth value is simply the deviation from north that faces the UAS when starts taking the first image of the 42-image series to build the spherical image.

To ensure that this error was independent of the LAI value for each sample point, the angle error (so the difference between true north rotation and the angle set in the first raw photo metadata) was plotted (figure 15).

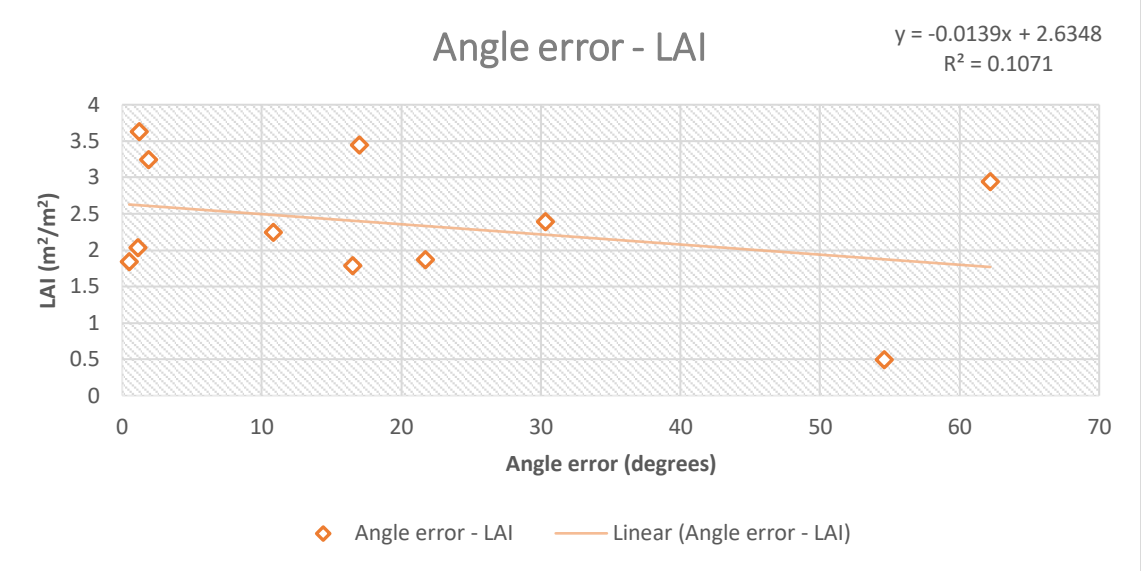

Fig. 15: Leaf Area Index (UAS-based) against angle error. [Source: own elaboration.]

Regression parameters and the plot itself show that the error is randomly distributed. Additionally, metadata from the final spherical image was analysed too. It was found that one of the angles that contained that metadata was very close to the camera YAW angle identified in the first raw image metadata.

Finally, when analysing the first raw image metadata, it was found that there were two YAW angles: camera and UAS. Despite being very close one to the other, it was finally used the camera YAW angle to study its relation to the north rotation, as it was considered to be the one that defines the final image characteristics, and moreover was the less deviated from the true north angle rotation (table 1).

Table 1: Angles extracted from metadata and rotation in the image editor. Units are degrees. [Source: own elaboration.]

POINT	ROTATION	CAMERA YAW	UAS YAW
P0	323	344.7	345.9
P1	115	131.5	132.5
P2	20	30.8	31.7
P3	62	92.3	93.5
P4	288	288.5	289.4
P6	78	79.9	81.3
P7	157	158.2	158.5
P8	158	215.2	215.8
P9	146	163	163
P10	17.4	18.5	18.6
P11	13	67.6	17.6

3.2. Vertical profiles of PAI

Two different vertical profiles were taken to make a preliminary study of the potentialities of this UAS to tale UAS-based hemispherical images from inside the canopy. An example of the hemispherical photos at different heights can be seen in the figure 16 below.

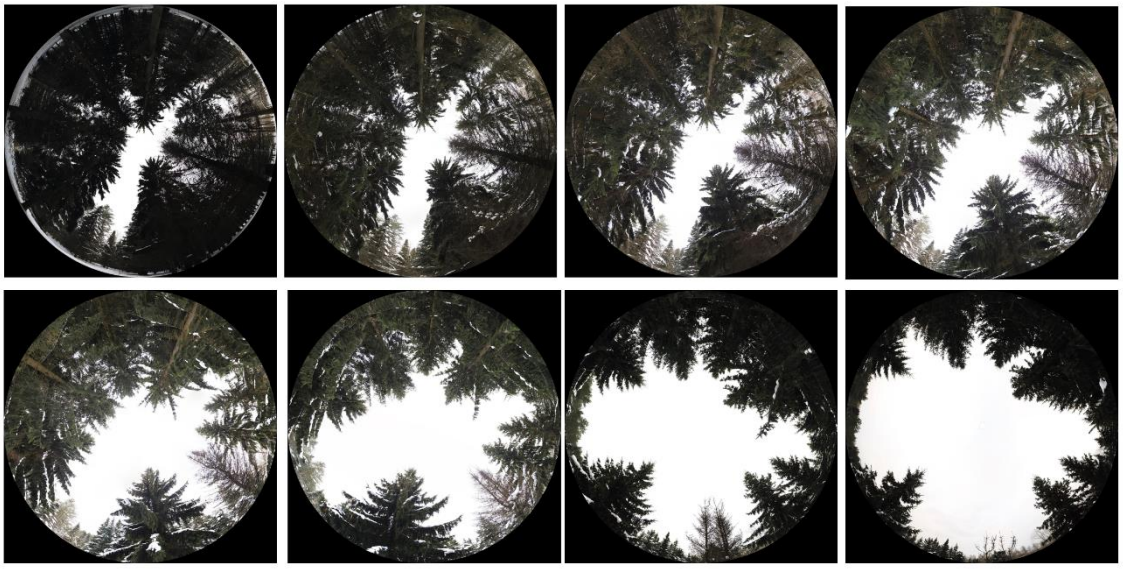

Fig. 16: Example of hemispherical photos of a vertical profile. In this case, from 0 meters to 14 m. [Source: own elaboration.]

After, these photos were analysed in Hemisfere. The results can be seen in next figures 17 and 18.

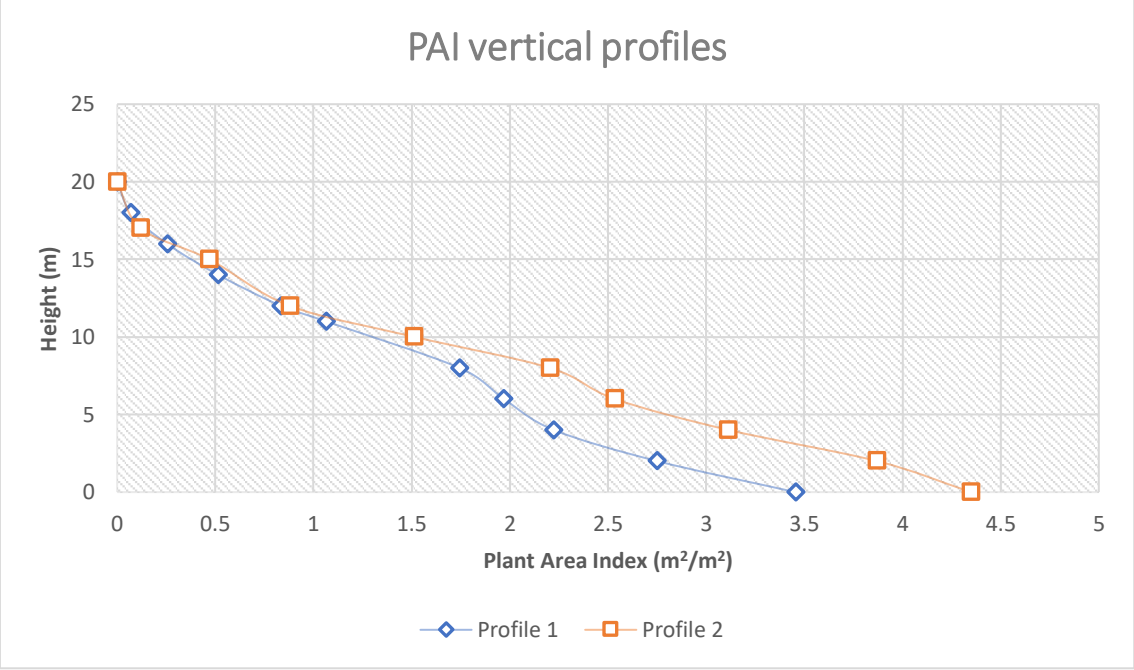

Fig. 17: Vertical profiles of Plant Area Index. [Source: own elaboration.]

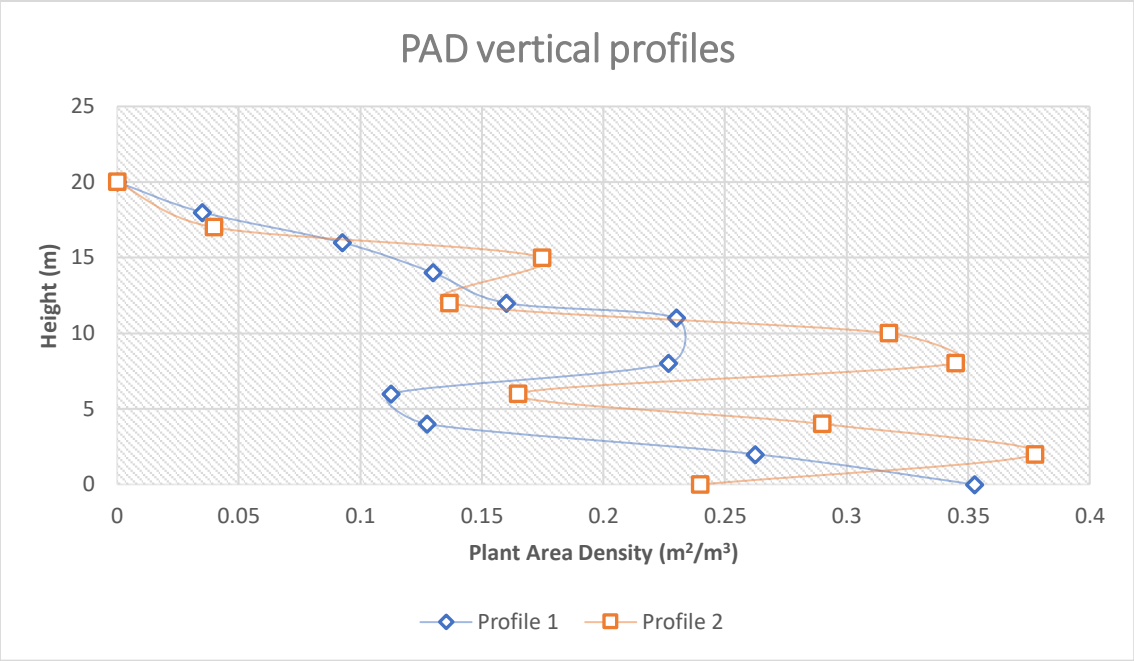

Fig. 18: Vertical profiles of Plant Area Density. [Source: own elaboration.]

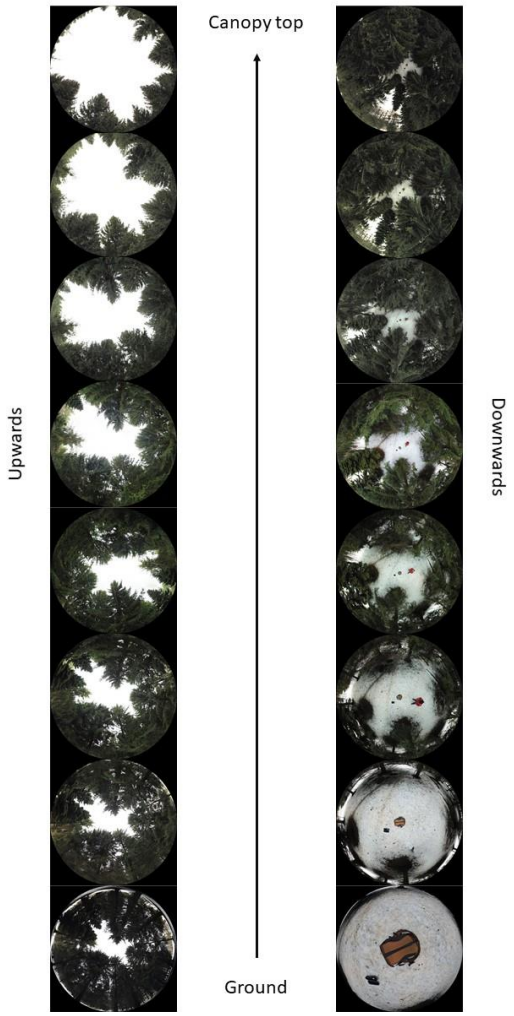

Fig. 19: Vertical profile of a spruce stand in Viikki Arboretum (in blue in figures 17 and 18). On the left, upward looking photos; on the right, downward looking photos. [Source: own elaboration.]

On the one hand, in the figure 17 it can be seen that, as expected, the Plant Area Index (PAI) reduces its value the more height the image is taken. This is logical because when the UAS is flying up, it gets closer to the sky, and therefore it leaves plant material below him, which will not be part of the PAI at that height.

On the other hand, figure 18 shows what is it known as the foliage profile, or in other words, the foliage density distribution throughout the canopy. In case of profile 1, it can be seen that in lower parts, the density is high, and it gets lower until 5 meters, then there is a sudden increase and then PAD diminishes until the canopy top.

This can be explained if it is taken into account the physical characteristics of the sample point where this vertical profile was taken. It was a spruce stand with lots of dead branches in the low part of the stem. These dead branches density diminished until proper crown base height, which can be assumed at 5 meters. From 5 meters to 15 meters there is a PAD peak, which can be supposed as the crown main core. From 10 meters to the top of the

canopy, there is a constant decrease of PAD, until it reaches the 0 value. This is logical, especially if it is beard in mind the spruce form, which is very conical, and therefore the crown reduction with height is very constant.

In orange, are shown the profiles for the second location. It can be seen that the PAI graph follows the same pattern of the one in the first location, which is logical as both profiles were taken in the same spruce stand, but in this case there is more PAI in the lower parts. However, in this second location, there were different trees of different heights: this can also be seen in the PAD graph. On this second location, there were much less branches in the lower part, then an important layer of dead branches and finally different trees of different heights. This would explain the different peaks in PAD.

To compare upward and downward looking photos, it was also used the Python code to create downward hemispherical photos at each flight height, by flipping them using an image editor (GIMP 2.10.22). The result can be seen in figure 19.

One direct result of this methodology is that it can be flown the UAS directly to the crown base height to estimate the LAI. This way, it would be estimating only non-woody LAI, and therefore it only would need the correction of the clumping index to obtain the true LAI.

4. DISCUSSION

4.1. UAS-based HP

In this thesis, it has been presented a new methodology to estimate forest canopy and light parameters using a recently released UAS, the Parrot ANAFI. This new method allows to take spherical photos at any height and in lots of different forest canopies. These spherical photos can be processed to create downward or upward looking hemispherical photos.

The only reference known at this moment of UAS-based upwards hemispherical photography is the work of Brüllhardt *et al.* (2020). In that case, they used a DJI S900 hexacopter, a UAS that weights 3.3 kg and has an approximate diameter of 1 meter. Additionally, they equipped the UAS on its top with the DHC.

Their objective was to fly the UAS through the canopy to take hemispherical photos at different heights and therefore represent a vertical profile of the foliage. After that, they validated those images with synthetic hemispherical pictures, derived from point clouds created with photogrammetric techniques. According to their work, despite the fact that comparison showed that the new methodology was accurate enough, they realized the difficulties of flying a UAS of those dimensions through a canopy. That is why they had to open specific gaps in the canopy by harvesting some trees to create enough space to take the vertical profile.

Also, the stability of the UAS was difficult to achieve and maintain due to its dimensions. General wind affected to the UAS inside the canopy and the propellers-produced wind affected the camera stabilization.

With the new Parrot ANAFI method presented in this thesis, this last two problems are solved, at least substantially. Firstly, because the size of the Parrot ANAFI is ideal to fly it through the canopy; and secondly because the problem of propellers destabilizing the camera disappears, as it is used the UAS camera itself. However, it is true that the general wind affects more the little UAS than the big one.

In this thesis, it is presented a method that shows a high correlation with the traditional digital hemispherical photography (R^2 = 0.80). Furthermore, the bias between the UAS-based photo and the DH photo is, except in 3 sample points, less than ±1, which is considered to be the accepted range of uncertainty ascribed to LAI measurements using optical techniques (Fernandes *et al*., 2003; Garrigues *et al*., 2008a; Camacho *et al*., 2013).

As it was presented in the results, the main deviation consists in a bias of Parrot ANAFI method comparing it to DHP. Nevertheless, this deviation can be attributed to a combination of three different issues: image resolution (which theoretically lowers DHC LAI), exposure (lower exposure is traduced in higher LAI), and the image projection. Exposure is known to be a very critical issue in indirect optical LAI measurements such as DHP, and yet it was followed a protocol in the photo acquisition, it always leads to a random subjectivity. But the third issue is also relevant. If the projection used in Hemisfer considers the central annulus bigger or smaller than it should be to recreate the reality, it is traduced into an less accurate estimation of LAI.

To adjust this exposure problem, a possible solution would be to take the photos in RAW format, as this format allows to modify the exposure once the image has been taken. In this case, the images that needed some correction were adjusted in a photo editor (Windows photo editor), as they were taken in jpg to make the process easier. Nevertheless, further research to study the relations between exposure, resolution, gap fraction and LAI is required.

An issue to be commented here too, is the fact that in this thesis the minimum and the maximum LAI output of Hemisfer have used to calculate an average. To further studies it would be useful to analyse separately each LAI output, and see if all the methods of LAI estimation that the software has have the same bias or not. However, as this process has been followed in both methods, the possible error is annulled.

This last phenomenon of annulled error also happens with the snow. As this thesis has been redacted in Helsinki in winter, some photos were taken where the conifer stands were covered in snow. Although it would lead to an overestimation of LAI, as both photos were taken at the same time, the comparison error is null.

Another aspect that has to be beard in mind is the positioning and Global Navigation Satelite System (GNSS) connection of the UAS. In this thesis, as the aim was to compare both methodologies from the ground, the positioning precision was not taken with absolute accuracy, as both techniques were used in the same spot. However, other works (Brawn *et al.,* 2015), used an additional GPS to ensure enough accuracy. They used a 10-meter resolution GPS, which resulted to work at a 5-meter resolution. The inner Parrot ANAFI GPS uses a module of less than 3 meters precision (GPS Module - U-BLOX UBX-M8030 GPS, 1.2 m of standard derivation according to the white manual of Parrot ANAFI), so much better. Nevertheless, other references can be found in which the UAS positioning precision is also incremented by different methods, such laser measures (Brüllhardt *et al.*, 2020).

Although in under-canopy situations GNSS signal is commonly degraded or entirely absent under dense forest conditions (Krisanski *et al.*, 2020), in this thesis, the positioning X-Y issue was considered non-relevant, and the Parrot ANAFI accuracy was accepted. It must be said that the flight stabilization and positioning stability of this UAS was surprisingly rigorous, at least in the tested locations. Nonetheless, for further research, it would be useful to study the viability of an optical positioning system, that would allow to know the relative position from a Ground Control Point, with centimetric accuracy.

4.2. Vertical profiles of PAI

As it was presented previously, one of the biggest advantages of the Parrot ANAFI in the vertical profiles acquirement is its size. All other references of UASs used inside the forest canopy are UASs of a weight at least of 1.4 kg (McNeil *et al.*, 2015; Brüllhardt *et al.,* 2020; Brown *et al.*, 2020; Krisanski *et al.*, 2020).

With a size and a weight much lower than all the other commercial UASs used in forest applications, this UAS can be perfectly used in clear to dense forest canopy conditions. In the data collection, as was stated in the measurements, it was important to look for a spot that had enough clear area for the UAS to complete a whole vertical ascension. However, this minimum size could be set to 10 – 15 m^2, whereas in the work of Brüllhardt *et al.* (2020), the minimum size needed for their UAS was of 180 m^2.

Very related to this last issue, it must also be stated than the manoeuvrability of this UAS was very positive. It was flown in the most controllable fight mode, so that the control of the pilot is maximized, as it was done in the work of Krsianski *et al.* (2020). In the same work, they had to deactivate the collision avoidance system, because it made impossible to fly the UAS through the canopy. The Parrot ANAFI does not include collision avoidance system, what is good precisely for this reason, as the pilot has the whole control of the UAS, but at the same time the whole responsibility is on the pilot. In this thesis, there were a couple of crashes, but it is something inherent to UASs, and specially UASs that work without collision systems inside a forest canopy. Therefore, crashes and associated frustration can be expected in these situations (McNail *et al.*, 2015).

Regarding the results, the LAD obtained values are logical in a spruce stand (Gspaltl *et al.*, 2013). Nonetheless, it can be seen that there are strong peaks in the LAD distribution of the crowns. Although it is true that those are a faithful reflect of the reality, it could also bee explained by two different aspects.

On the one hand, photos could be negatively affected by the differential exposure in the ascension. If figure 16 is analysed, it can be seen that the light conditions of each photo is not the same. Although it was tested in some photos by modifying the light and see the effects on the PAD profile, there was not observed a substantial reduction of the peaks. However, for further research it should be interesting to manually adjust the exposure of all the UAS-based hemispherical photos and keep that set exposure constant in all the ascension, as underexposure of canopy elements should depend only on sky brightness (Brüllhardt *et al.*, 2020).

On the other hand, as PAD is calculated by differential PAI in relation to the height steps of each PAI layer, the precision of measurement of the height is an important aspect to bear in mind. In this thesis, it was used the information of the log files to confirm that the height was the correct one. According to the white manual of Parrot ANAFI, height is calculating using all the sensors that the UAS is equipped with inertial measurement unit (with gyroscope and accelerometer), magnetometer, GPS, ultrasonar and barometer. As the barometer height estimation is well known (Li *et al.*, 2013), a combination of all the sensors is supposed to have a very high accuracy.

It must be said here that in the data collection for this thesis, there were times that the UAS suddenly stopped working: the error message was "the motors of the UAS stopped working". Researching about this, it was found that may be the unmatching information of the GPS and the other sensors could cause this problem. Nevertheless, this problem still remains low studied.

Finally, it is obvious that the more layers of PAI are acquired, the more precision and reliability would have the final PAD profile. In Brüllhardt *et al.* (2020) work, they use between 5 and 10 photos in each 2-meter step.

5. CONCLUSIONS

In this document, it has been shown that Parrot ANAFI has a great potential as a new innovative tool to estimate forest parameters. Due to its small size and thanks to its integrated high-quality camera, spherical images taken from inside the canopy can be a very powerful but easy way of extracting information from the forest. Here, the studied parameters have been only related to leaf parameters, such as Leave or Plant Area Index and Leaf or Plant Area Density. Nevertheless, spherical images are an important way of estimating other type of forest parameters, such as basal area, stand density or even local photosynthetic indexes. Furthermore, despite it is true that this new tool can be as good as traditional digital hemispherical photography, and even better if time efficiency is taken into consideration, the potential of this UAS-based DHP is not restricted only to ground photography. In fact, it is in the capability of this little UAS to fly through the canopy that resides its biggest capacities.

In the presented document, it has been studied how this UAS model can be flown through the canopy, taking photos at any height and therefore with capability of analysing the whole vertical profile of the forest, from ground to above canopy. However, it is obvious that this methodology has limitations, as in very dense forests with no gaps in the canopy the UAS cannot be flown throughout the complete vertical. Despite this, it is true that this new method developed has a huge potential, as the combination of its size, weight, and easy-control, is traduced in a very sensible improve over all other UAS-based hemispherical photography in the reviewed literature. Nevertheless, further research by studying possible reasons for the deviations in the final LAI values has to be done.

Until now, it is known that there are three main issues that can lead to the observed bias: resolution, although lower resolution seems to produce higher LAI as gap fraction is overestimated; exposure, as underexposed images tend to produce higher LAI and vice versa; and the projection of the images, or in other words, the lens parameters used in Hemisfer, as the projection of the annulus is a key factor in the general LAI estimation. The calibration of both cameras and the introduction of the correspondent parametrization in Hemisfer would be an interesting start to continue the started research in this document.

Nowadays, most LAD profiles of a forest canopy are derived from laser scanning data (Laser Imaging Detection and Raging, or LIDAR) or from a point cloud derived from photogrammetric techniques. This document presents a new, independent and more economically affordable method to estimate LAI or PAI throughout the canopy, and therefore being able to estimate a LAD or PAD vertical profile (i.e. foliage distribution) without depending on expensive and normally dependant on third parties technology such as LIDAR.

It is true, though, that some progresses should be done in order to optimize the use of the Parrot ANAFI UAS in forest environment. For example, the GPS exactitude would be recommended to improve, as it may be needed more precision in the location system that the one offered by the inner software. A good GPS connection is traduced in more flight stability and therefore in a safer flight experience and image quality, and accordingly, in more data reliability. Also, more research in the location of the north in the hemispherical images is needed in order to broaden the use of this new technique for example to light environment analysis.

However, it must be said that for a UAS that is basically sold as a toy, the amount of scientific work that can be done with it makes this tool totally worth it for forest research.

6. ACKNOWLEDGEMENTS

I want to specially thank my supervisor Jonathan Atherton for his constant help and advice. Thanks also to Albert Porcar-Castell, and all the personnel involved in the Optics and Photosynthesis Laboratory, for trusting me and lending me all the material needed for accomplish this thesis. Thanks to Jaana Bäck and all the Research Group members for embrace me in the team as one more.

7. REFERENCES

Abdollahnejad, A., Panagiotidis, D., Surový, P., Ulbrichová, I., 2018. *UAV capability to detect and interpret solar radiation as a potential replacement method to hemispherical photography.* Remote sensing 10 (2018) 423. https://doi.org/10.3390/rs10030423 [Consulted: 09/03/2021]

Agus Umarhadi, D. and Danoedoro, P., 2020. *Comparing canopy density measurement from UAV and hemispherical photography: an evaluation for medium resolution of remote sensing-based mapping.* International Journal of Electrical and Computer Engineering 11 (1), 356-365 DOI: 10.11591/ijece.v11i1.pp356-364 [Consulted: 08/03/2021]

Agus Umarhadi, D., Danoedoro, P., Wicaksono, P., Widayani, P., Widayani, P., Nurbandi, W., Juniansah, A., 2018. *The comparison of canopy density measurement using UAV and Hemispherical Photography for remote sensing based mapping.* Conference: 2018 4th International Conference on Science and Technology (ICST)At: Yogyakarta, Indonesia, Indonesia. DOI: 10.1109/ICSTC.2018.8528670 [Consulted: 08/03/2021]

Ambrosia, V. G., Wegener, S. S., Sullivan, D. V., Buechel, S. W., Brass, J. A., Dunagan, S. E., et al., 2002. *Demonstrating UAV-Acquired Real-Time Thermal Data over Fires*. Photogrammetric Engineering and Remote Sensing 69 (4): 391-402. https://www.asprs.org/wp-content/uploads/pers/2003journal/april/2003_apr_391-402.pdf [Consulted: 08/03/2021]

Andis Arietta, A.Z., 2020. *Evaluation of hemispherical photos extracted from smartphone spherical panorama images to estimate canopy structure and forest light environment*. BioRxiv The Preprint Server For Biology. https://doi.org/10.1101/2020.12.15.422956 [Consulted: 22/03/2021]

Asner, P.G., Scurlock, J.M.O., Hicke, J., 2003. *Global synthesis of leaf area index observations: implications for ecological and remote sensing studies.* Global ecology and Biogeography 12 (2003) 191-205. https://doi.org/10.1046/j.1466-822X.2003.00026.x [Consulted: 09/03/2021]

Banu, T.P., Borlea, G.F., Banu, C., 2016. *The use of drones in forestry.* Journal of Environmental Science and Engineering B 5 (2016) 557-562. http://www.davidpublisher.org/index.php/Home/Article/index?id=30060.html [Consulted: 09/03/2021]

Bechschäfer, P., Seidel, D., Kleinn, C., Xu, J., 2013. *On the exposure of hemispherical photographs in forests.* iForest - Biogeosciences and Forestry 6 (2013) 228 – 237. http://www.sisef.it/iforest/contents/?id=ifor0957-006 [Consulted: 08/03/2021]

Brown, L.A., Suthernland, D.H., Dash, J., 2020. *Low-cost unmanned aerial vehicle-based digitl hemispherical photography for estimating leaf area index: a feasibility assessment.*

International Journal of Remote Sensing 41 (23) 9064-9074. https://doi.org/10.1080/2150704X.2020.1802527 [Consulted: 09/03/2021]

Brüllhardt, M., Rotach, P., Schleppi, P., Bugmann, H., 2020. *Vertical light transmission profiles in structured mixed deciduous forest canopies assessed by UAV-based hemispherical photography and photogrammetric vegetation height models.* Agricultural and Forest Meteorology 281 (2020) 107843. https://doi.org/10.1016/j.agrformet.2019.107843 [Consulted: 09/03/2021]

Camacho, F., J. Cernicharo, R. Lacaze, F. Baret, and M. Weiss., 2013. *GEOV1: LAI, FAPAR Essential Climate Variables and FCOVER Global Time Series Capitalizing over Existing Products. Part 2: Validation and Intercomparison with Reference Products.* Remote Sensing of Environment 137 (October): 310–329. https://doi.org/10.1016/j.rse.2013.02.030 [Consulted: 08/03/2021]

Chen, J.M., 1996. *Optically-based methods for measuring seasonal variation in leaf area index of boreal conifer forests*. Agriculture and Forestry Meteorology, 80 (2-4), 135–163. https://doi.org/10.1016/0168-1923(95)02291-0 [Consulted: 08/03/2021]

Chen, J.M., Black, T., 1992. *Defining leaf area index for non-flat leaves*. Plant Cell Environ. 15, 421–429. https://doi.org/10.1111/j.1365-3040.1992.tb00992.x [Consulted: 08/03/2021]

Chen, J.M., Govind, A., Sonnetang, O., Zhang, Y., Barr, A., Amiro, B., 2006. *Leaf are index measurements at Fluxnet-Canada forest sites.* Agricultural and Forest Meteorology 140 (2006) 257-268. https://doi.org/10.1016/j.agrformet.2006.08.005 [Consulted: 08/03/2021]

Chen, J.M., Menges, C.H., Leblanc, S.G., 2005. *Global mapping of foliage clumping index using multi-angular satellite data.* Remote Sensing of Environment 97 (2005), 447-457. https://doi.org/10.1016/j.rse.2005.05.003 [Consulted: 08/03/2021]

Chen, J.M., Rich, P.M., Gower, S.T., Norman, J.M., Plummer, S., 1997. *Leaf area index of boreal forests: theory, techniques, and measurements*. J. Geophys. Res. 102 (1984–2012), 29429–29443. DOI: 10.1029/97JD01107 [Consulted: 08/03/2021]

Chianucci, F. and Cutini, A., 2012. *Digital hemispherical photography for estimating forest canopy properties: current controversies and opportunities*. iForest – Biogeosciences and Forestry 5(6). DOI: https://doi.org/10.3832/ifor0775-005 [Consulted: 08/03/2021]

Cui, L., Jiao, Z., Zhao, K., Sun, M., Dong, Y., Yin, S., Li, Y., Chang, Y., Guo, J., Xie, R., Zhu, Z., Li, S., 2020. *Retrieval of vertical foliage profile and leaf area index using transmitted energy information derived from ICESat GLAS data.* Remote sensing 12 (2020) 2457. https://doi.org/10.3390/rs12152457 [Consulted: 09/03/2021]

Danson, F.M., Hetherington, D., Morsdorf, F., Koetz, G., Allgöwer, B., 2007. *Forest canopy gap fraction from terrestrial laser scanning.* IEEE Geoscience and remote sensing letters 4 (1). https://ieeexplore.ieee.org/document/4063287 [Consulted: 09/03/2021]

Èermák, J., 1998. *Leaf distribution in large trees and stands of the floodplain forest in southern Moravia.* Tree Physiology 18 (11) 727-737. https://doi.org/10.1093/treephys/18.11.727 [Consulted: 09/03/2021]

Fernandes, R., C. Butson, S. Leblanc, and R. Latifovic., 2003. *Landsat-5 TM and Landsat-7 ETM+ Based Accuracy Assessment of Leaf Area Index Products for Canada Derived from SPOT-4 VEGETATION Data.* Canadian Journal of Remote Sensing 29 (2): 241–258. https://doi.org/10.5589/m02-092 [Consulted: 08/03/2021]

Garrigues, S., R. Lacaze, F. Baret, J. T. Morisette, M. Weiss, J. E. Nickeson, R. Fernandes, et al. 2008. *Validation and Intercomparison of Global Leaf Area Index Products Derived from Remote Sensing Data*. Journal of Geophysical Research 113 (G02028). https://doi.org/10.1029/2007JG000635 [Consulted: 08/03/2021]

Glatthorn, J. and Bechkschäfer, P., 2014. *Standardizing the protocol for hemispherical photographs. Accuracy assessment of binarization algorithms.* PloS ONE 9 (11) e111924. https://doi.org/10.1371/journal.pone.0111924 [Consulted: 09/03/2021]

Gonsamo, A., Pellikka, P., 2009. *The computation of foliage clumping index using hemispherical photography.* Agricultural and Forest Management 149 (10) 1781-1787. https://doi.org/10.1016/j.agrformet.2009.06.001 [Consulted: 09/03/2021]

Gspaltl, M., Bauerle, W., Binklew, D., Sterba, H., 2013. *Leaf area and light use efficiency patterns of Norway spruce under different thinning regimes and age classes.* Forest Ecology and Management 288 (2013) 49-59. https://doi.org/10.1016/j.foreco.2011.11.044 [Consulted: 09/03/2021]

Guangjian, Y., Ronghai, H., Jinghui, L., Marie, W., Halian, J., Xihan, M., Donghui, X., Wuming, Z., 2019. *Review of indirect optical measurements of leaf area index: Recent advances, challenges, and perspectives.* Agricultural and Forest Meteorology 265 (2019) 390-441. https://doi.org/10.1016/j.agrformet.2018.11.033 [Consulted: 09/03/2021]

Itakura, K. and Hosoi, F., 2020. *Automatic tree detection from Tree-Dimensional images reconstructed from 360° spherical camera using YOLO v2.* Remote Sensing 12 (6), 988 https://doi.org/10.3390/rs12060988 [Consulted: 08/03/2021]

Jain, M., Kuriakose, G., Balakrishnan, R., 2010. *Evaluation of methods to estimate foliage density in the understorey of a tropical evergreen forest.* Current science 98 (4). https://www.jstor.org/stable/24111702?seq=1 [Consulted: 09/03/2021]

Khokthong, W., Clara Zemp, D., Irawan, B., Sundawati, L., Kreft, H., Hölscher, D., 2019. *Drone-based assessment of canopy cover for analyzing tree mortality in an oil palm agroforest.* Frontiers for Global Change 2(12). https://doi.org/10.3389/ffgc.2019.00012 [Consulted: 08/03/2021]

Krisanski, S., Taskhiri, M.S., Turner, P., 2020. *Enhancing Methods for Under-Canopy Unmanned Aircraft System Based Photogrammetry in Complex Forests for Tree Diameter Measurement*. Remote sensing 12 (2020) 1652. https://doi.org/10.3390/rs12101652 [Consulted: 09/03/2021]

Leblanc, S.G., Chen, J.M., Fernandes, R., Deering, D.W., Conley, A., 2005. *Methodology comparison for canopy structure parameters extraction from digital hemispherical photography in boreal forests.* Agriculture and Forest Meteorology 129 (2005) 187-2007. https://doi.org/10.1016/j.agrformet.2004.09.006 [Consulted: 09/03/2021]

Majasalmi, T., 2015. *Estimation of leaf area index and the fraction of absorbed photosynthetically active radiation in a boreal forest.* PhD Thesis, Department of Forest Sciences, Faculty of Agriculture and Forestry, University of Helsinki. Dissertationes Forestales 187. https://dissertationesforestales.fi/pdf/article1970.pdf [Consulted: 09/03/2021]

Mäkela, A., Pulkinen, M., Kolari, P., Lagergren, F., Berbigier, P., Lindroth, A., Loustau, D., Nikinmaa, E., Vesala, T., Hari, P., 2007. *Developing an empirical model of stand GPP with the LUE approach: analysis of eddy covariance data at five contrasting conifer sites in Europe.* Global

Change Biology 14 (1): 92-108. https://doi.org/10.1111/j.1365-2486.2007.01463.x [Consulted: 08/03/2021]

McNeil, B.E., Pisek, J., Lepisk, H., Flamenco, E.A., 2016. *Measuring leaf angle distribution in broadleaf canopies using UAVs.* Agricultural and Forest Meteorology 218-219 (2016) 204-208. https://doi.org/10.1016/j.agrformet.2015.12.058 [Consulted: 09/03/2021]

Nilson, T., 1971. *A theoretical analysis of the frequency of gaps in plant stands*. Agricultural Meteorology 8 (1971) 25-38. https://doi.org/10.1016/0002-1571(71)90092-6 [Consulted: 22/03/2021]

Ollero, A., and Merino, L., 2006. *Unmanned Aerial Vehicles as Tools for Forest-Fire Fighting*. Forest Ecology and Management 234 (1): 263-74. DOI: 10.17265/2162-5263/2016.11.007 [Consulted: 08/03/2021]

Parrot ANAFI Product Sheet. Parrot Drones SAS – RCP Paris 808 408 704. https://www.parrot.com/assets/s3fs-public/2020-07/bd_anafi_productsheet_en_210x297_2018-06-04.pdf [Consulted: 08/03/2021]

Parrot ANAFI White Paper Manual. Parrot Drones SAS – RCP Paris 808 408 704. https://www.parrot.com/assets/s3fs-public/2020-07/white-paper_anafi-v1.4-en.pdf [Consulted: 08/03/2021]

Roberti Alves de Almeida, D., Stark, S.C., Shao, G., Schietti, J., Nelson, B.W., Silva, C.A., Gorgens, E.B., Valbuena, R., De Almeida Papa, D., Santin Brancalion, Henrique., 2019. *Optimizing the remote detection of tropical rainforest structure with airborne lidar: leaf area profile sensitivity to pulse density and spatial sampling.* Remote Sensing 11 (2019) 92. https://doi.org/10.3390/rs11010092 [Consulted: 09/03/2021]

Ruder, M., Dosovitskiy, A., Brox, T., 2018. *Artistic style transfer for videos and spherical images.* International Journal of Computer Vision 126 (2018) 1199-1219. https://doi.org/10.1007/s11263-018-1089-z [Consulted: 09/03/2021]

Ryu, Y., Nilson, T., Kobayashi, H., Sonnentag, O., E. Law, B., D.Baldocchi, D., 2010. *On the correct estimation of effective leaf area index: Does it reveal information on clumping effects?.* Agricultural and Forest Meteorology 150 (2010) 463-472. https://doi.org/10.1016/j.agrformet.2010.01.009 [Consulted: 08/03/2021]

Sanusi, R., Johnstone, D., May, P., Livesley, S.J., 2017. *Microclimate benefits that different street tree species provide to sidewalk pedestrians relate to differences in Plant Area Index.* Landscape and Urban Planning 157 (2017) 502-511. https://doi.org/10.1016/j.landurbplan.2016.08.010 [Consulted: 09/03/2021]

Sumida, A., Nakai, T., Yamada, M., Ono, K., Uemura, S. & Hara, T. 2009. *Ground-based estimation of leaf area index and vertical distribution of leaf area density in a* Betula ermanii *forest. Silva Fennica* 43 (5) 799–816. https://silvafennica.fi/article/174 [Consulted: 09/03/2021]

Tan, C.-W., Zhang, P.-P., Zhou, X.-X., Wang, Z.-X., Xu, Z.-Q., Mao, W., Li, W.-X., Huo, Z.-Y., Guo, W.-S., Yun, F., 2020. *Quantitative monitoring of leaf area index in wheat of different plant types by integrating NDVI and Beer-Lambert law*. Nature, Scientific Reports 10 (929). https://doi.org/10.1038/s41598-020-57750-z [Consulted: 09/03/2021]

Uribe, D., Mattar, C., Camacho, F., 2018. *Estimación de parámetros biofísicos de la vegetación en praderas y cultivos en Chile mediante fotografía digital hemisférica obtenidas por una cámara GoPro.* Revista de Teledetección, AET 52 (2018), 1-15. https://doi.org/10.4995/raet.2018.9315 [Consulted: 09/03/2021]

Wang, H., 2019. *Estimating forest attributes from spherical images.* Master of Science in Forestry, Faculty of Forestry and Environmental Management, University of New Brunswick. http://ifmlab.for.unb.ca/LabPubs/theses/WangHZ2020a.pdf [Consulted: 09/03/2021]

Wang, H., Yang, T.R., Waldy, J., Kershaw, J.A., JR., 2021. *Estimating individual tree heights and DBHs from vertically displaced spherical image pairs.* Mathematical and Computational Forestry and Natural-Resources Sciences 13 (0) 0-13. https://www.researchgate.net/publication/348634350_Estimating_Individual_Tree_Heights_and_DBHs_from_Vertically_Displaced_Spherical_Image_Pairs [Consulted: 09/03/2021]

Wang, W.-M., Li, Z.-L., Su, B.-H., 2007. *Comparison of leaf angle distribution functions: effects on extinction coefficient and fraction of sunlit foliage.* Agricultural and Forest Meteorology 143 (1-2) 106-122. https://doi.org/10.1016/j.agrformet.2006.12.003 [Consulted: 09/03/2021]

Weiss, M., Baret, F., Smith, G.J.; Jonckheere, I., Coppin, P., 2004. *Review of methods for in situ leaf area index (LAI) determination Part II. Estimation of LAI, errors and sampling.* Agricultural and Forest Meteorology 121 (2004) 37-53. https://doi.org/10.1016/j.agrformet.2003.08.001 [Consulted: 09/03/2021]

Zhao, F., Yang, X., Schull, M.A., Román-Colón, M.O., Yao, T., Wang, Z., Zhang, Q., Jupp, D.L.B., Lovell, J.L., Culvenor, D.S., Newnham, G.J., Richardson, A.D., Ni-Meister, W., Schaaf, C.L., Woodcock, C.E., Strahler, A.H., 2011. *Measuring effective leaf area index, foliage profile, and stand height in New England forest stands using a full-waveform ground-based lidar.* Remote Sensing of Environment 115 (11). https://doi.org/10.1016/j.rse.2010.08.030 [Consulted: 09/03/2021]

Zheng, G. and Moskal, L.M., 2009. *Retrieving Leaf Area Index (LAI) sing Remote Sensing: theories, methods and sensors.* Sensors 9 (2009) 2719-2745. https://doi.org/10.3390/s90402719 [Consulted: 09/03/2021]

Zhu, X., Skidmore, A.K., Wang T., Liu, J., Darvishzadeh, R., Shi, Y., Premier, J., Heurich, M., 2018. *Improving leaf area index (LAI) estimation by correcting for clumping and woody effects using terrestrial laser scanning.* Agricultural and Forest Meteorology 263 (2018) 276-286. https://doi.org/10.1016/j.agrformet.2018.08.026 [Consulted: 09/03/2021]